Energy 77 (2014) 352–361

Contents lists available at ScienceDirect

Energy

journal homepage: www.elsevier.com/locate/energy

A thermodynamic study of hot syngas impurities in steel reheating furnaces – Corrosion and interaction with oxide scales

H. Liu [a,b], M. Saffaripour [b,*], P. Mellin [b], C.-E. Grip [c], W. Yang [b], W. Blasiak [b]

[a] State Key Laboratory of Coal Combustion, Huazhong University of Science and Technology, Wuhan, Hubei 430074, China
[b] Division of Energy and Furnace Technology, KTH Royal Institute of Technology, Brinellvägen 23, S-100 44 Stockholm, Sweden
[c] Division of Energy Science, Luleå University of Technology, 971 87 Luleå, Sweden

A R T I C L E I N F O

Article history:
Received 27 March 2014
Received in revised form
30 July 2014
Accepted 27 August 2014
Available online 17 October 2014

Keywords:
Reheating furnace
Thermodynamic calculation
Syngas
Impurities
Alkali compounds

A B S T R A C T

Environmental concerns lead industries to implement gasified biomass (syngas) as a promising fuel in steel reheating furnaces. The impurities of syngas as well as a combination with iron oxide scale form complex mixtures with low melting points, and might cause corrosion on steel slabs. In this paper, the effects of syngas impurities are thermodynamically investigated, when scale formation on the steel slabs surface simultaneously takes place. A steel reheating furnace can be divided into preheating, heating, and soaking zones where the temperature of a steel slab changes respectively. Therefore, the thermodynamic calculation is performed at different temperatures to predict the fate of impurities. Then, the stable species are connected with respective zones in a reheating furnace. It is concluded that reactions due to alkali compounds, chloride, and particulate matter could take place on steel slabs. In the low temperature range, interaction of sodium chloride occured with pure iron prior to scale formation. Then, at high temperature the reactions of impurities are notable with iron oxides due to scale growing. Furthermore, the multicomponent reactions with syngas impurities showed that most of alkali contents evaporate at first stages, and only small amounts of them remain in slag at high temperature.

© 2014 Elsevier Ltd. All rights reserved.

1. Introduction

Due to energy intensity, the steel industries are nominated as one of the main sectors of CO_2 emissions in the world. On average, 1.8 tons of CO_2 are emitted for every ton of steel production. For example, in 2010 the steel industry accounted for approximately 6.7% of total global CO_2 emissions [1,2]. Reheating furnaces produce 69.5 kg/ton CO_2 during the steel production [2]. Such emissions can be reduced by numerous methods of combustion and gasification such as oxy-fuel ignition up to 50 percent as reported in Ref. [3].

Fuel switching could be one of the possible solutions to reduce CO_2 emissions. Several ongoing projects exist to implement syngas as primary fuel for different facilities like boilers [4–6]. Nevertheless, the potential effects of syngas are not investigated as fuel for reheating furnaces. Therefore, prior to direct usage of syngas it is needed to investigate the possible effects of impurities on steel products.

Generally, gasification of biomass is a promising technique, which was developed from various aspects during the past decades [7–9]. In order to produce syngas from gasified biomass, temperature should range between 800 and 1200 °C [10]. The syngas composition varies, depending on different fuel types of biomass such as raw, wood chips, pellets, and torrefied [11,12]. The flue gases of syngas are consisted of several impurities such as most common alkali metals like potassium (K) and sodium (Na), halogens like chlorine (Cl), particulate matter, tar, sulfur compounds, and other contaminants [13,14]. These alkali contents due to chemical reactions with iron and iron oxides form complex scale layers, which can cause corrosion and slagging in a temperature that corresponds to reheating furnace.

Syngas combustion, in the case of reheating furnace, provides an effective way to avoid ash deposition on the steel slabs because of presence of alkali metals/chlorides in gas phase at high temperature. To date, the fate of alkali species in gasification has not been investigated extensively than in combustion, and there are few actual measurements of gas phase alkali concentrations [15–17]. For example, an online hot gas analysis by Molecular Beam Mass Spectrometry (MBMS) was done for three different kinds of biomass to see the effects of alkali metals [18]. Inorganic compounds such as alkali metals and mineral particles could be measured to serve input data for thermodynamic equilibrium calculations [19]. However, from the total alkali contents of a given

---

* Corresponding author. Tel.: +46 8 790 85 31; fax: +46 8 20 76 81.
E-mail address: mohsensp@kth.se (M. Saffaripour).

http://dx.doi.org/10.1016/j.energy.2014.08.092
0360-5442/© 2014 Elsevier Ltd. All rights reserved.

solid biomass, only a minor fraction remains in the gas phase after the gasification process [20,21]. At the same time, some of such compounds melt or even vaporize above 600 °C, and can leave the reactor as aerosols and vapors, respectively [22].

The objective of this study is to investigate ash formation due to challenges of syngas as an alternative fuel in steel reheating furnaces. Syngas is presented as fuel that has a smaller amount of ash content, and comprehensive thermodynamic calculation is done based on effects of impurities on scale formation. The compounds under investigation (alkali metals, halogens and particulate matter) are more likely to react with steel slabs surface in the reheating furnace. The thermodynamic of reactions based on global equilibrium approach is provided by FactSage 6.2 [23] to evaluate the possible formation of compounds, not considering transport phenomena such as condensation, deposition, diffusion and melting behavior (temperature and speciation) of the condensable species. The data is presented as behavior of impurities and as potential negative effects of alkali contents on steel surfaces according to low and high temperature variations regarding the reheating furnace zones.

In this paper, we look at the effects of impurities, which are provided by combustion of syngas fuel in steel reheating furnace. First, a background is given with reheating furnace, and scale formation due to syngas flue gases, after that the thermodynamic model, and finally the results are presented.

2. Reheating furnace

The purpose of reheating furnaces is to heat up the steel slabs to a target temperature and maintain it until its profile becomes uniform and any carbide has been dissolved by diffusion. The target temperature can range from around 1000 to 1250 °C depending on to the hot-rolling behavior of various steel alloys [24].

Reheating furnaces are often fuel fired, and as a result, the fuel creates oxygen-bearing gases (H_2O, CO_2, and O_2) in the combustion chamber. The steel slab at ambient temperature (27 °C) is charged in the furnace during the reheating process and passes through different zones (preheating, heating, and soaking) continuously to reach the target temperature as shown in Fig. 1. When the steel alloy has reached desirable temperature, the slab is discharged from the furnace and further processed by descaling as cold water is sprayed over it.

3. Scale formation procedure

Previous findings show that the oxidation during isothermal gravimetric experiments is controlled by two main mechanisms [25,26]. Initially, when the steel sample was almost scale free, the oxidation was found to be governed by mass transfer of oxygen through the gas boundary layer to the sample surface. When the scale becomes thicker, the rate mechanism changes, and the diffusion of ions through the layers becomes much more important. Oxide scale formation is important as heat transfer by radiation to slabs is enhanced by a low surface emissivity. In addition to safety concerns, this is the main reason why an oxidizing atmosphere is preheated. Moreover, because of the aggressive oxidizing reaction, severe mass losses often in the range of 1–2% are reported for carbon steels [27].

During the reheating procedure, temperature, gas composition, and residence time are the main parameters that are responsible for the extent of scaling of slabs in a furnace. At first, the stocks are charged in an oxidized atmosphere of flue gases with 3% extra oxygen as shown in Fig. 2. Then, the oxidation of scale starts only when a certain temperature is reached, at least 800 °C. Finally, the time for scaling is about 2–2½ hours in a reheating furnace. As shown in Fig. 2, gaseous alkali species in the furnace atmosphere will condense on cold slabs at about 800 °C, silicates and CaO/MgO are left as dust and bombard the surface. Surface scale begins to grow significantly up to temperature of more than 1000 °C, and a thin layer of alkali containing compounds (oxides, carbonates, chlorides, or sulphates) is formed. In addition, some dust of silicates and CaO/MgO lie loosely on the surface. As the scale grows, the outer surface may react with dusts of silicates and CaO/MgO. However, gas phase alkali compounds are less likely to react at this stage. A change can be expected that the silicates become more fluid at higher temperature, which can possibly increase the tendency to stick to the subject.

Fig. 3 shows the scale growth in relation to the different zones of the reheating furnace. The temperature was measured by thermocouples drilled into a slab passing through the reheating furnace in a Swedish plate mill [28]. The difference of the thermocouple data between and above skid indicates the shadowing effect of such skid. The picture can be also used to outline the natural reaction sequence of ash forming elements behavior in a reheating furnace.

4. Methodology of thermodynamic model

Theoretically, thermodynamics provides a powerful method to calculate the reaction process related to a given system at

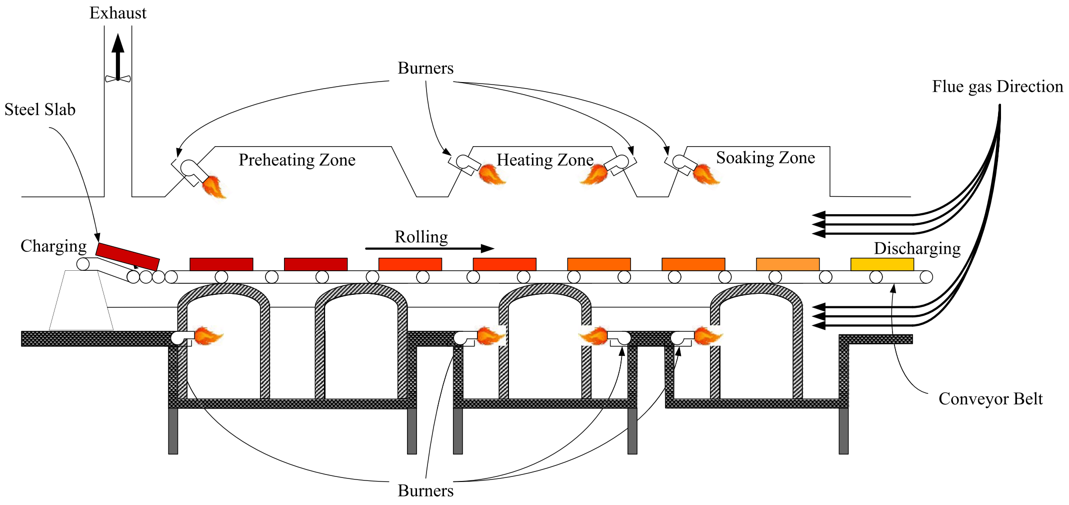

Fig. 1. Schematic of reheating furnace.

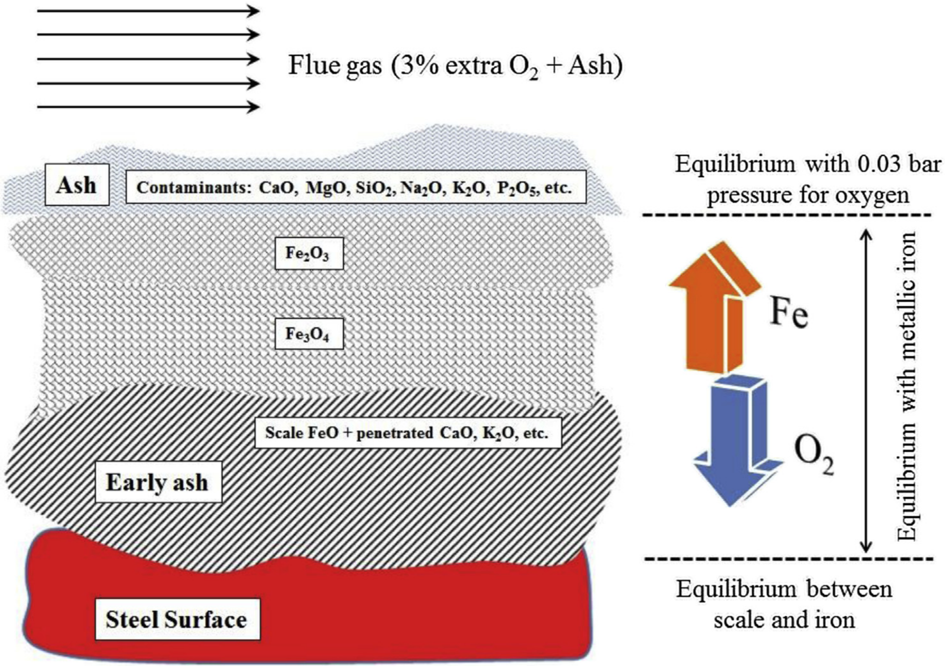
Flue gas (3% extra O_2 + Ash)
Ash
Contaminants: CaO, MgO, SiO_2, Na_2O, K_2O, P_2O_5, etc.
Fe_2O_3
Fe_3O_4
Scale FeO + penetrated CaO, K_2O, etc.
Early ash
Steel Surface
Equilibrium with 0.03 bar pressure for oxygen
Fe
O_2
Equilibrium with metallic iron
Equilibrium between scale and iron

Fig. 2. Schematic of possible behaviors of ash lying on the steel slab.

equilibrium. Equilibrium calculations by FactSage 6.2 are based on minimization of Gibbs energy. When the parameters, such as the elementary composition of the fuel and air, temperature and pressure have been specified, this software package will search the species including these elements from the database. This database is consisted of series of information, calculation, and manipulation modules that enable one to easy access to substances and solution database. The difficulty will arise when the results of the equilibrium calculation are compared with those of real combustion systems. It should be clear the applicability of a global equilibrium model to practical combustors has several limitations. A direct comparison of these results with experimental data is not possible without additional experimental information about local salt compositions. The main limitations of this method are listed as the following statements:

- Equilibrium may not be attained for all species in real systems due to kinetics effects.
- No temperature or concentration gradient is taken into account.
- Physical processes (i.e. adsorption) are not taken into account.
- Results are extremely dependent on the database (reliability of the thermodynamic data).
- Original modes of occurrence are not included (only elemental composition).

However, most of these drawbacks can be suppressed at least partly, by taking simple assumptions.

Modeling strategy is defined in accordance with temperature variation in the reheating furnace. The transition from low to high temperature is interrelated consequently to preheating, heating, and soaking zone as shown in Table 1. It has to be mentioned that

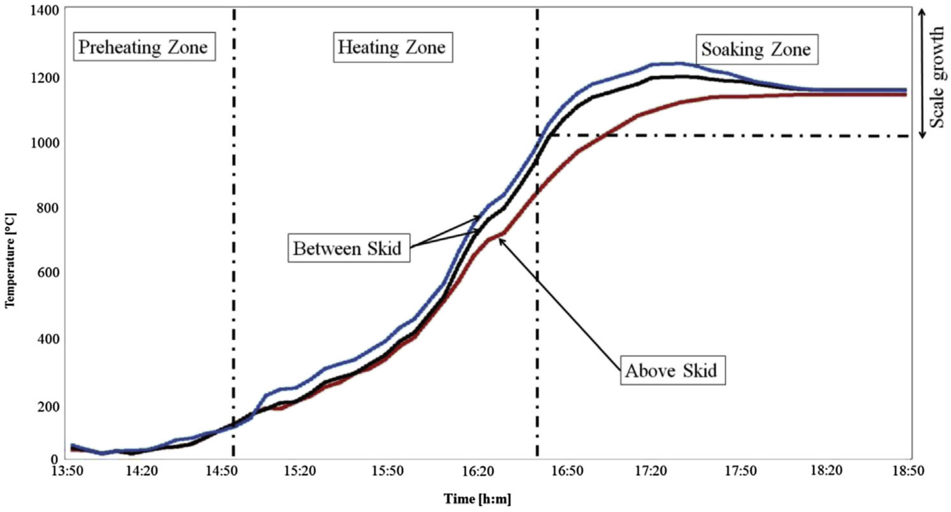

Fig. 3. Heating profile in slab during reheating process [28].

temperature of steel slab surface assumed to be uniform in each zone.

In this work, thermodynamic equilibrium calculations have been conducted to investigate the preliminary phenomena and reaction mechanisms as follow:

- The transformation of alkali species, distribution in gas/solid phases under different conditions (possibility of condensation, deposition, evaporation, and melting)
- The heterogeneous reactions among Fe, Fe-oxides, K, Na, Cl and mineral compounds including Si, Ca, Al
- The effect of impurities on oxide scale formation process and steel properties, as well as potential risk when using syngas in steel preheating furnace reasonably.

5. Results and discussions

The effects of impurities are presented as two main scenarios that would be interesting for alkali species and fine particle interaction with steel slabs. The first one is at relative low temperature, where scale does not appear obviously, and the other is at higher temperature, when scale formation turns out to be thicker as shown in Fig. 3.

5.1. Low temperature corrosion

For the first step in the thermodynamic calculation modeling, the low temperature interaction is interrelated to the preheating zone. The preheating zone encompasses the temperature range between 427 and 727 °C. Low temperature corrosion is generally faced when some region in the system operates below the dew point temperature of the molten ashes. However, the dew point temperature is not always known, or possible to estimate closely. An interesting research by Nielsen et al. [29] suggests an array of problems, which is an outcome of certain conditions in the combustion chamber and in the flue gas system.

The molten ash in flue of syngas condenses in regions with low temperature. However, as long as facilities operate above the condensation temperature, the risk of ash deposition is largely avoided. For instance, in order to investigate the low temperature alkali contents reactions, the reactants consisting of NaCl and Fe under simulated gas atmosphere ($15\%CO_2 + 3\%O_2 + 72\%N_2 + 10\% H_2O$) were chosen to ascertain the possible reactions between NaCl and Fe. Fig. 4 presents the most species in products related to Fe. It seems that the oxidation of Fe is dominant at 427 °C, but at higher temperature (727 °C) Cl primarily forms a solution with Fe. At this phase, negligible scale starts to form; however, NaCl will actually be in contact with pure Fe.

$$2NaCl + 2Fe + 2O_2 \rightarrow Na_2Fe_2O_4 + Cl_2 \tag{1}$$

$$6NaCl + 8Fe + 6O_2 \rightarrow 3Na_2Fe_2O_4 + 2FeCl_3 \tag{2}$$

It means that, both $FeCl_x$ ($x = 2, 3$) and FeOCl formation is negligible, and this phenomenon may attribute to the low concentration of HCl. On the other hand, actually, if NaCl penetrates into the metal matrix, reaction between NaCl and Fe may also occur by means of reactions (1) and (2) according to the literature [30].

5.2. High temperature multicomponent interaction

At high temperature, alkali contents are not just the main source of interactions with iron oxides but also the particulates matter could form mineral mixtures. Eutectic sodium and potassium salts in the ash material can melt at gasification temperatures above 800 °C as shown in Table 2. Unlike solid particulates, which can be separated by physical means such as barrier filters, vaporized alkali compounds will remain in the product gas at high temperature, and thus cannot always be removed by simple filtration. Condensation of the vaporized alkali typically begins at approximately 900 °C on particles in the gas stream, with subsequent deposition on cooler surfaces.

Fig. 5 shows a combination of potassium-involved reactions at different temperatures regarding to reheating furnace. Results present if SiO_2 and Al_2O_3 are introduced into the system of $K_2O–Fe_2O_3$, an interesting phenomenon can be detected, in which K_2O can combine with Al_2O_3, SiO_2 forming aluminosilicate, prior to Fe_2O_3. Furthermore, the products vary according to the temperature, and $KAlSiO_4$ will decompose at high temperature. The main reactions can be characterized by reactions (3)–(7). In fact, the similar results observed when KCl is introduced to reactants system containing SiO_2 and Al_2O_3 (by replacing K_2O with KCl in calculation). It can be concluded that the addition of SiO_2 and Al_2O_3 promotes the transformation of KCl to K-silicates (seeing reactions (8)–(12)). Furthermore, FeO originated by the decomposition of Fe_2O_3, can react with Al_2O_3, and SiO_2 to form $FeAl_2O_4$, $FeSiO_3$, Fe_2SiO_4 by the reactions (13)–(16), which is undesirable because products containing FeO often result to low temperature melting points [31].

$$K_2O + Al_2O_3 + 2SiO_2 \rightarrow 2KAlSiO_4 \tag{3}$$

$$K_2O + Al_2O_3 \rightarrow 2KAlO_2 \tag{4}$$

$$KAlSiO_4 \rightarrow KAlO_2 + SiO_2 \tag{5}$$

$$K_2O + SiO_2 \rightarrow K_2SiO_3 \tag{6}$$

$$KCl_{(s)} \rightarrow KCl_{(g)} \tag{7}$$

$$KCl + H_2O \rightarrow KOH + HCl \tag{8}$$

Table 1
Strategy of the study in a reheating furnace.

Study (phase)	Method	Involved species	Corresponding zone	Temperature range (°C)
1. (Low temperature corrosion)	Thermodynamic modeling	Fe + impurities in syngas flow	Preheating zone	427–727
2. (High temperature multicomponent interaction)	Thermodynamic modeling	Fe_2O_3 + alkali chloride (NaCl/KCl) Fe_2O_3 + Mixed minerals ($Na_2O/K_2O/SiO_2/Al_2O_3/CaO$)	Heating/soaking zone	727–1227
3. (Evaporation)	Thermodynamic modeling	Fe + NaCl/KCl	All zones	427–1227
4. (Kinetic effects)	Discussion	Ions	All zones	427–1227

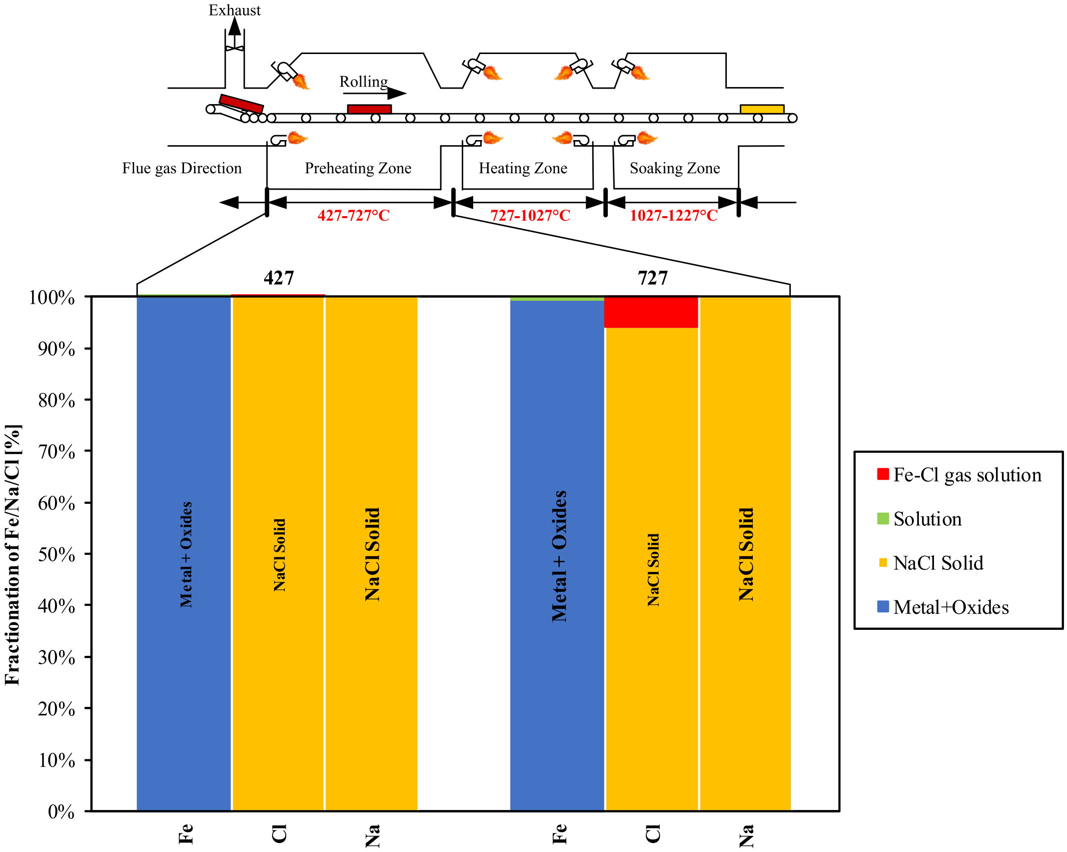

Fig. 4. Fractionation of Fe, Cl and Na in the case of NaCl being added to the thermodynamic system of flue gases and Fe, at atmospheric pressure.

$$2KOH + Al_2O_3 + 2SiO_2 \rightarrow 2KAlSiO_4 + H_2O \quad (9)$$

$$2KOH + Al_2O_3 + 4SiO_2 \rightarrow 2KAlSi_2O_6 + H_2O \quad (10)$$

$$2KOH + Al_2O_3 \rightarrow 2KAlO_2 + H_2O \quad (11)$$

$$Fe_2O_3 + 2HCl \rightarrow 2FeOCl + H_2O \quad (12)$$

$$Fe_2O_3 \rightarrow FeO + O + Fe_3O_4 \quad (13)$$

$$FeO + Al_2O_3 \rightarrow FeAl_2O_4 \quad (14)$$

$$FeO + SiO_2 \rightarrow FeSiO_3 \quad (15)$$

$$2FeO + SiO_2 \rightarrow Fe_2SiO_4 \quad (16)$$

Additionally, K_2O also can be involved in the reaction with CaO and SiO_2, and complex minerals will form. By doping SiO_2 and CaO into the system of $K_2O–Fe_2O_3$, we can find CaO is inclined to combine with Fe_2O_3, while K_2O is inclined to combine with SiO_2(see Fig. 5). Compared with newly formed silicate, the formation of calcium ferrite is at higher temperature. The main reactions have been summarized by reactions (17)–(23).

At low temperature (below 800 °C):

$$CaO + SiO_2 \rightarrow CaSiO_3 \quad (17)$$

$$K_2O + 2SiO_2 \rightarrow K_2Si_2O_5 \quad (18)$$

$$K_2O + SiO_2 \rightarrow K_2SiO_3 \quad (19)$$

At high temperature (above 800 °C):

$$CaO + 2Fe_2O_3 \rightarrow CaFe_4O_7 \quad (20)$$

$$CaO + Fe_2O_3 \rightarrow CaFe_2O_4 \quad (21)$$

$$2CaO + Fe_2O_3 \rightarrow Ca_2Fe_2O_5 \quad (22)$$

$$K_2O + SiO_2 \rightarrow K_2SiO_3 \quad (23)$$

It seems that the interaction between Fe_2O_3 and K_2O is not remarkable, no new products generated by the reaction of K_2O and Fe_2O_3.

In contrast to K_2O, Na_2O is more active, and a little $Na_2Fe_2O_4$ formed by reaction (24) above 1027 °C as it is shown in Fig. 6. Furthermore, another possible product can be found from the phase diagram Na–Fe–O which is presented in Fig. 7. Obviously, Na_2O can react with both FeO and Fe_2O_3 to form different mineral solutions such as $Na_2Fe_2O_4$, $2NaFeO_2$, $2Na_3FeO_3$, and Na_4FeO_3. Due to the Fe_2O_3 and FeO consumed, it is expected that oxidation loss increases as more oxides form.

$$Na_2O + Fe_2O_3 \rightarrow Na_2Fe_2O_4 \quad (24)$$

(usually it can be written as: $Na_2O \cdot Fe_2O_3$)

$$Na_2O + Fe_2O_3 \rightarrow 2NaFeO_2 \quad (25)$$

$$3Na_2O + Fe_2O_3 \rightarrow 2Na_3FeO_3 \quad (26)$$

$$2Na_2O + FeO \rightarrow Na_4FeO_3 \quad (27)$$

The calculation results suggested at high temperature, new minerals including Fe and alkali metals (K/Na) as well as Fe chloride

Table 2
Melting/eutectic temperatures for different pure species and binary mixtures with Fe [31].

System	Melting/eutectic temperatures (°C)	Composition at eutectic point (mole % alkali)
NaCl	801	
KCl	772	
$FeCl_2$	677	
$FeCl_3$	300	
NaCl–$FeCl_2$	370–374	~56
NaCl–$FeCl_3$	151	45.3
KCl–$FeCl_2$	340–393	45.8–91.8
KCl–$FeCl_3$	202–202	24–47

forms in reactants system of Fe_2O_3 as shown in Fig. 8. Simultaneously, NaCl or KCl evaporated and formed HCl, and Na(K)OH in addition to gaseous NaCl or KCl.

In other literature [33,34], we can get more information about the behavior of NaCl and KCl lying on the heating surface in boiler system, and the induced corrosion by KCl and NaCl could be well interpreted by reaction (28). It can be seen that the diffusion of chloride ions plays an important role in oxidation of Fe.

$$2NaCl_{(s,l)} + Fe_2O_{3(s)} + \frac{1}{2}O_{2(g)} \rightarrow Na_2Fe_2O_{4(s,l)} + Cl_{2(g)} \qquad (28)$$

It should be reminded that behavior of NaCl and KCl in deposition layer in boiler happens at lower temperature than that in preheating zone of reheating furnace. Thus, it is recommended that most of KCl and NaCl will evaporate in the heating and soaking zones of steel reheating furnace.

5.3. Evaporation

Generally, the driving force for the condensation is the ability of the surface to lead away the heat as well as the partial pressure of molten ashes in relation to solubility limits in the gas phase. The complexity of ash deposits from gas phase is complex and not yet fully understood. Therefore, the phenomenon of evaporation of existence impurities in syngas usually occurs for the temperature range of the whole furnace.

It has been confirmed that alkali species usually can be captured by aluminosilicates [35], which indicates that bauxite, bentonite, and kaolinite are excellent adsorbents for the removal of K_2O and KCl. In other words, potassium is easy to be bonded with Si and Al. Of course, there are some other potential products related to different reactants composition of K_2O–SiO_2–Al_2O_3, which are listed as following: KAl_9O_{14}, $K_2Al_{12}O_{19}$, Al_2SiO_5, $KAlSi_2O_6$, $KAlSi_3O_8$, $KAlSiO_4$, and $K_2Si_2O_5$ in Fig. 9.

Figs. 10 and 11 describe calculation results on phase transformation of KCl and NaCl respectively at different temperatures in simulated flue gas atmosphere. It can be found that both KCl and NaCl evaporate slowly above 727 °C, and the evaporation rate increases rapidly at 927 °C, which indicates quite a few KCl or NaCl will change to gaseous alkali species from solid state. As regards to

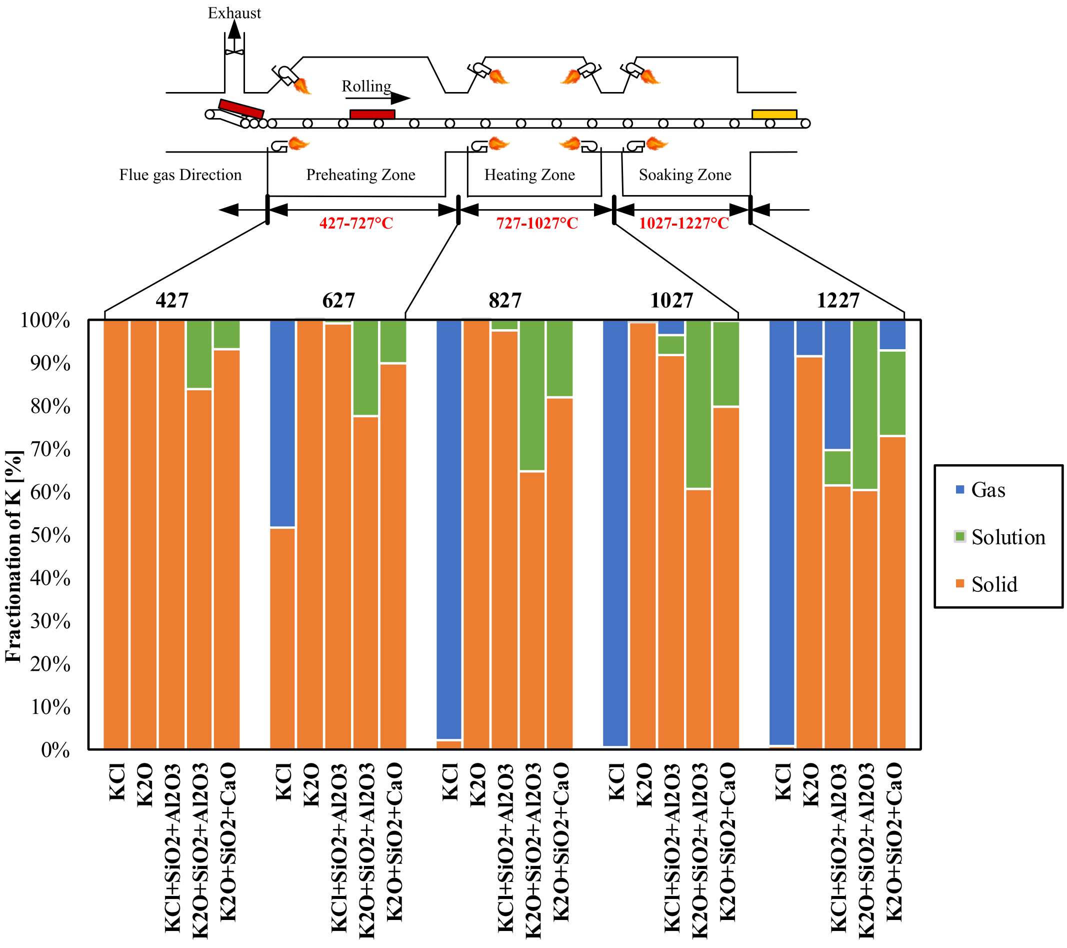

Fig. 5. Fractionation of K in cases where different K-containing impurities are being added to the thermodynamic system of flue gases and Fe_2O_3, at atmospheric pressure.

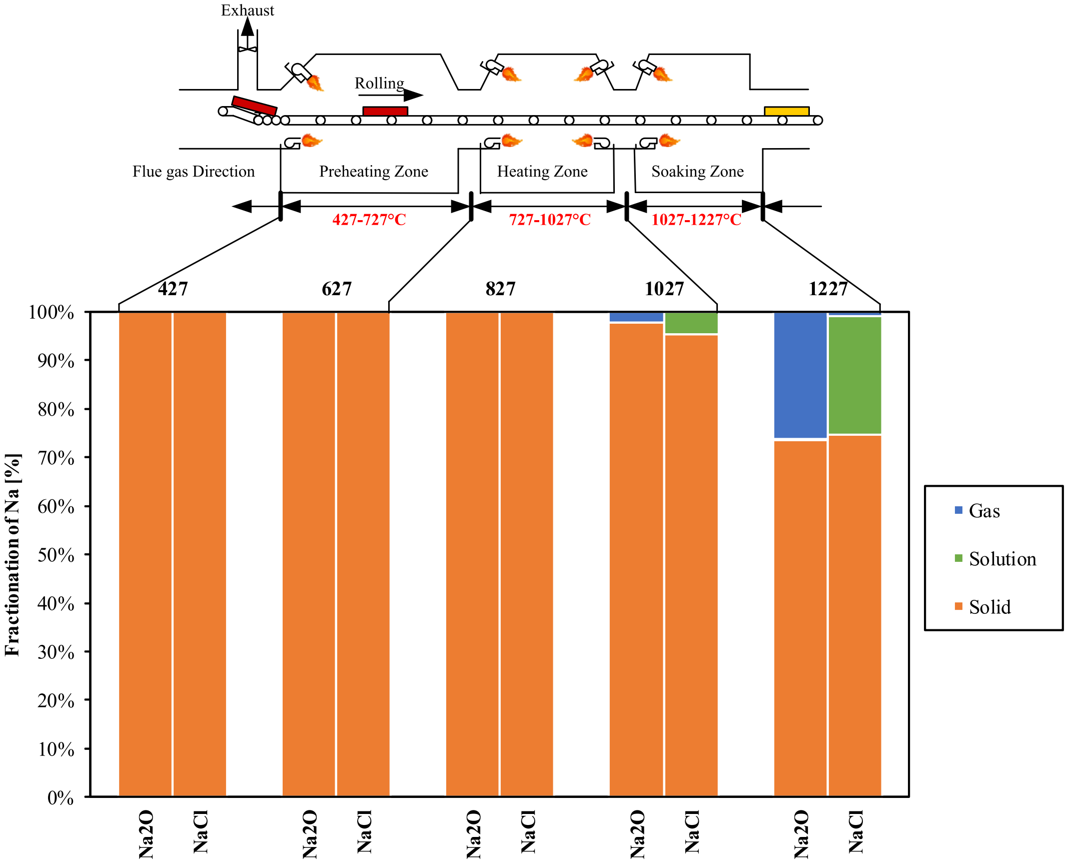

Fig. 6. Fractionation of Na in cases where different Na-containing impurities are being added to the thermodynamic system of flue gases and Fe_2O_3, at atmospheric pressure.

the distribution of gaseous species, besides $RCl_{(g)}$ or $RCl_{2(g)}$, $ROH_{(g)}$ also has been found, but its amount is very low. The formation of $ROH_{(g)}$ can be explained by reactions (29) and (30), where, R represents K or Na.

$$RCl_{(s)} \rightarrow RCl_{(g)} \tag{29}$$

$$RCl_{(g)} + H_2O_{(g)} \rightarrow ROH_{(g)} + HCl_{(g)} \tag{30}$$

It is noted that actual evaporation temperature of KCl and NaCl may vary according to the local condition, while it goes without saying that at the heating and soaking zones, for KCl or NaCl lying on the surface of steel, it is likely to evaporate.

Additionally, comprehensive work is needed to determine the similar behaviors of other species such as K_2O/Na_2O, K_2SO_4/Na_2SO_4 etc.

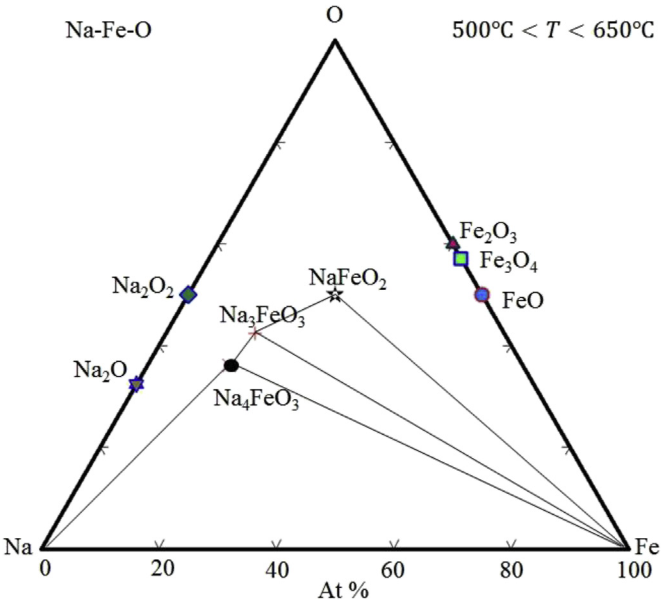

Fig. 7. A sketch of principal occurring phases in the three phase Na–Fe–O [32].

5.4. Kinetic effects

The calculations in this work are based on equilibrium. In reality, kinetic diffusion can affect the outcome results. The effect of chloride ion diffusion on Fe oxidation has already been mentioned. Some further examples are listed as following sentences:

- The dust in the gas phase is often enough, and has a composition to cause trouble with lining on scale, but probably a big part of it does not react with steel surface. Therefore, such dust follows the gas through the whole volume of furnace.
- During combustion, the flame shape is expected to be influenced if we have slow burning material. Probably, the combustion products leaving the flame are in equilibrium. However, when the flame cools, evaporated compounds do not always have time to react back with the solid or liquid dust, so that gas phase and mineral dust pass the furnace separately. The effect of this on reaction with slab surface can be illustrated by looking at Figs. 5, 6, and 8. Additionally, different reactions occur if only evaporated alkali metals are exposed to the surface or if they react together with Al_2O_3 or $SiO_2 + Al_2O_3$.

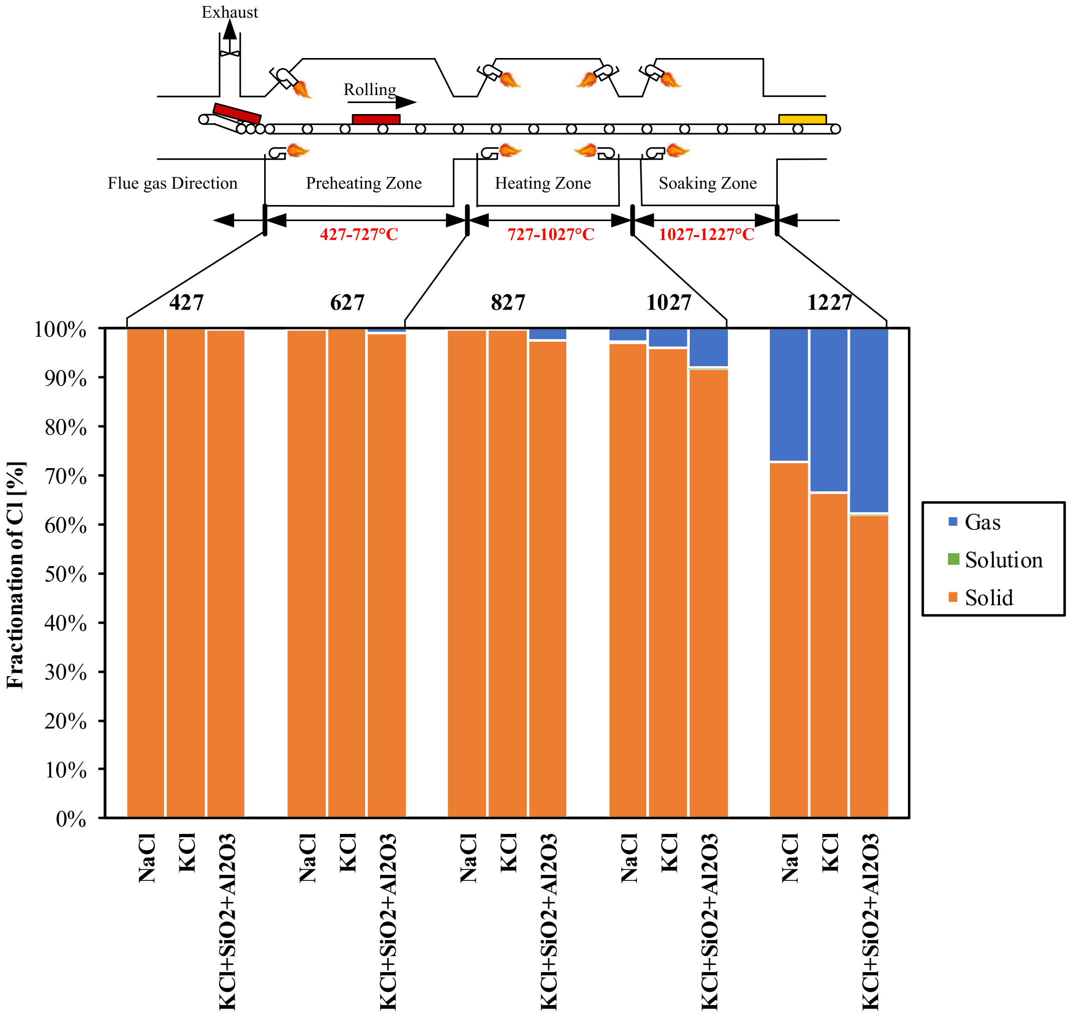

Fig. 8. Fractionation of Cl in cases where different Cl-containing impurities are being added to the thermodynamic system of flue gases and Fe_2O_3, at atmospheric pressure.

6. Conclusion

Gasification of biomass has identified as the most promising way to use syngas for steel reheating furnace in term of clean fuel with less ash contents. The conclusion can be summarized by the following paragraphs.

- In early preheating zone, calculations indicate that Cl compounds are more reactive than Na ones. When the temperature increases formation of Fe-oxides is favored compared to interaction with alkali metals/chloride.
- In the late preheating up to soaking zones, by increasing the temperature iron oxides react with ash compounds to form solid

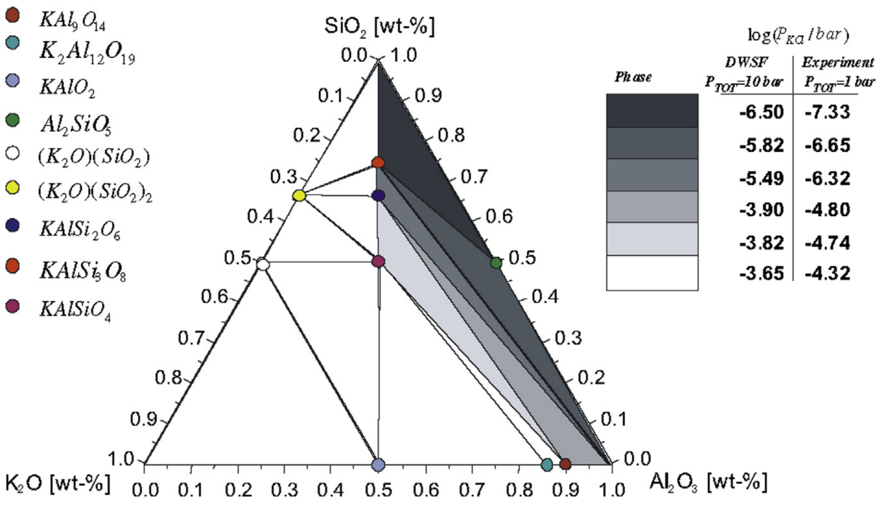

Fig. 9. Partial pressure of KCl over aluminosilicates depending on their composition [35].

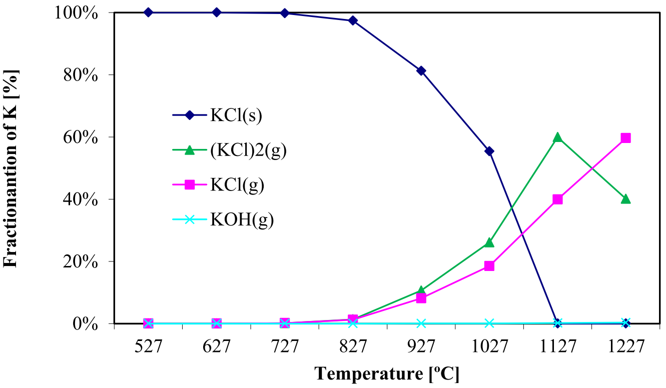

Fig. 10. Phase transformation of KCl at different temperatures (initial reactants composition: 1 mol (15%CO_2 + 3%O_2 + 72%N_2 + 10%H_2O) + 1 mol KCl(s), Pressure = 1 atm).

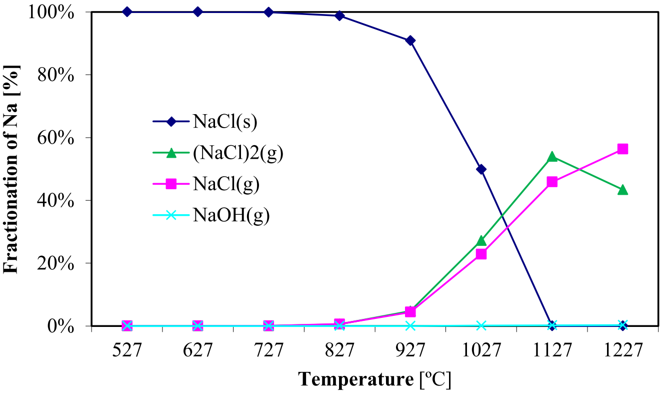

Fig. 11. Phase transformation of NaCl at different temperatures (initial reactants composition: 1 mol (15%CO_2 + 3%O_2 + 72%N_2 + 10%H_2O) + 1 mol NaCl(s), Pressure = 1 atm).

solutions. In this region, sodium is more prone to form such solutions compared to potassium, when the oxide scale (Fe_2O_3) is formed. The calculations show that Na in both NaCl and Na_2O reacts with Fe_2O_3, thus giving $(Na_2O) \cdot (Fe_2O_3)$, such solutions are known to have low melting point.

- In heating and soaking zones, by addition of mineral mixtures such as K_2O, SiO_2, Al_2O_3, and CaO the risk of solution formation and favored steel scaling is increased. It is observed that the most important particulates are SiO_2 and Al_2O_3, because of the formation of aluminasilicates, which increase solid solutions on steel slabs. In the actual case where more components might exist and the interaction may be very complex as well.
- In heating and soaking zones, as far as Cl is concerned, increase in temperature even in the presence of aluminasilicates, negligible amounts of solution will form.
- The evaporation of alkali metals and alkali chlorides starts at about 827 °C and is completed at about 1077 °C, which can make a circulation between evaporation and condensation in all zones.

Acknowledgments

The authors of this paper would like to thank funding through the Swedish Steel Producer's Association (Jernkontoret), from the Swedish Energy Agency (contract no. 35386-1). Additional financial support from FAZA RAZ Consulting Company and the Nature Science Foundation of China (51276074) are also acknowledged.

References

[1] IEA (International Energy Agency). World energy outlook, ISBN 978 92 64 08624 1.

[2] Battaglia V, Malfa E, Zanusso U, Arribas Ramirez JJ, Ekman T, Adler W, et al. EUR 25004-CO_2 reduction in reheating furnaces (CO2RED). Luxembourg: Publications Office of the European Union Research Fund for Coal and Steel Series; 2011, ISBN 978-92-79-21760-9. http://dx.doi.org/10.2777/91701. ISSN: 1831-9424.

[3] Von Schéele Joachim. Oxyfuel combustion in the steel industry: energy efficiency and decrease of CO_2 emissions. In: Palm Jenny, editor. Energy efficiency, ISBN 978-953-307-137-4.

[4] Calvo LF, Gil MV, Otero M, Morán A, García AI. Gasification of rice straw in a fluidized-bed gasifier for syngas application in close-coupled boiler-gasifier systems. Bioresour Technol 2012;109:206–14. http://dx.doi.org/10.1016/j.biortech.2012.01.027.

[5] Piotr H, Janusz L, Katarzyna M. Biomass gasification and Polish coal-fired boilers for process of reburning in small boilers. J Central South Univ 2013;20(6):1623–30. http://dx.doi.org/10.1007/s11771-013-1655-z.

[6] Kalisz S, Pronobis M, Baxter D. Co-firing of biomass waste-derived syngas in coal power boiler. Energy 2008;33(12):1770–8. http://dx.doi.org/10.1016/j.energy.2008.08.001.

[7] Huang Z, He F, Zheng A, Zhao K, Chang S, Zhao Z, et al. Synthesis gas production from biomass gasification using steam coupling with natural hematite as oxygen carrier. Energy 2013;53:244–51. http://dx.doi.org/10.1016/j.energy.2013.02.068.

[8] Møllera CB, Roknia M, Elmegaarda B, Ahrenfeldt J, Henriksen UB. Decentralized combined heat and power production by two-stage biomass gasification and solid oxide fuel cells. Energy 2013;58:527–37. http://dx.doi.org/10.1016/j.energy.2013.06.046.

[9] Raman P, Ram NK, Gupta R. A dual fired downdraft gasifier system to produce cleaner gas for power generation: design, development and performance analysis. Energy 2013;54:302–14. http://dx.doi.org/10.1016/j.energy.2013.03.019.

[10] Karamarkovic R, Karamarkovic V. Energy and exergy analysis of biomass gasification at different temperatures. Energy 2010;35(2):537–49. http://dx.doi.org/10.1016/j.energy.2009.10.022.

[11] Prins MJ, Ptasinski KJ, Janssen FJJG. More efficient biomass gasification via torrefaction. Energy 2006;31(15):3458–70. http://dx.doi.org/10.1016/j.energy.2006.03.008.

[12] Chen WH, Chen CJ, Hung CI, Shen CH, Hsu HW. A comparison of gasification phenomena among raw biomass, torrefied biomass and coal in an entrained-flow reactor. Appl Energy 2013;112:421–30. http://dx.doi.org/10.1016/j.apenergy.2013.01.034.

[13] Woolcock PJ, Brown RC. A review of cleaning technologies for biomass-derived syngas. Biomass Bioenergy 2013;52:54–84. http://dx.doi.org/10.1016/j.biombioe.2013.02.036.

[14] Niska J, Grip CE, Mellin P. Investigating potential problems and solutions of renewable fuel use in steel reheating furnaces. In: Proceeding of the Finnish–Swedish Flame Days; 2013.

[15] Turn SQ, Kinoshita CM, Ishimura DM, Hiraki TT, Zhou J, Masutani SM. An experimental investigation of alkali removal from biomass producer gas using a fixed bed of solid sorbent. Ind Eng Chem Res 2011;40(8):1960–7. http://dx.doi.org/10.1021/ie000749i.

[16] Wei X, Schnell U, Hein K. Behavior of gaseous chlorine and alkali metals during biomass thermal utilization. Fuel 2005;84(7–8):841–8. http://dx.doi.org/10.1016/j.fuel.2004.11.022.

[17] Salo K, Mojtahedi W. Fate of alkali and trace metals in biomass gasification. Biomass Bioenergy 1998;15(3):263–7. http://dx.doi.org/10.1016/S0961-9534(98)00019-1.

[18] Bläsing M, Chiavaroli G, Müller M. Influence of the particle size on the release of inorganic trace elements during gasification of biomass pellets. Fuel 2013;111:791–6. http://dx.doi.org/10.1016/j.fuel.2013.03.073.

[19] Froment K, Defoort F, Bertrand C, Seiler JM, Berjonneau J, Poirier J. Thermodynamic equilibrium calculations of the volatilization and condensation of inorganics during wood gasification. Fuel 2013;107:269–81. http://dx.doi.org/10.1016/j.fuel.2012.11.082.

[20] Erbel C, Mayerhofer M, Monkhouse P, Gaderer M, Spliethoff H. Continuous in situ measurements of alkali species in the gasification of biomass. Proc Combust Inst 2013;34(2):2331–8. http://dx.doi.org/10.1016/j.proci.2012.06.037.

[21] Aravind PV, Jong WD. Evaluation of high temperature gas cleaning options for biomass gasification product gas for solid oxide fuel cells. Prog Energy Combust Sci 2012;38(6):737–64. http://dx.doi.org/10.1016/j.pecs.2012.03.006.

[22] Baxter LL, Miles TR, Miles Jr TR, Jenkins BM, Milne T, Dayton D, et al. The behavior of inorganic material in biomass-fired power boilers, field and laboratory experiences. Fuel Process Technol 1998;54(1–3):47–78. http://dx.doi.org/10.1016/S0378-3820(97)00060-X.

[23] Bale CW, Chartrand P, Degterov SA, Eriksson G, Hack K, Mahfoud RB, et al. FactSage thermochemical software and databases. Calphad 2002;26(2):189–228. http://dx.doi.org/10.1016/S0364-5916(02)00035-4.

[24] Han SH, Chang D, Huh C. Efficiency analysis of radiative slab heating in a walking-beam-type reheating furnace. Energy 2011;36(2):1265–72. http://dx.doi.org/10.1016/j.energy.2010.11.018.

[25] Wilkström P, Weihong Y, Blasiak W. The influence of oxide scale on heat transfer during reheating of steel. Steel Res Int 2008;79(10). ISSN: 1611-3683: 765–75. http://dx.doi.org/10.2374/SRI08SP009.

[26] Wikström P, Blasiak W, Berntsson F. Estimation of the transient surface temperature and heat flux of a steel slab using an inverse method. Appl Therm Eng 2007;27(14–15):2463–72. http://dx.doi.org/10.1016/j.applthermaleng.2007.02.005.

[27] Chan DYL, Yang KH, Lee JD, Hong GB. The case study of furnace use and energy conservation in iron and steel industry. Energy 2010;35(4):1665–70. http://dx.doi.org/10.1016/j.energy.2009.12.014.

[28] Leden B, Wessberg NE. Improved energy efficiency in reheating furnaces by means of improved control. Jernkontorets forskning, report D 799. 2003-11-24. http://www.jernkontoret.se/ladda_hem_och_bestall/publikationer/stalforskning/rapporter/d799.pdf.

[29] Nielsen HP, Frandsen FJ, Dam-Johansen K. Lab-scale investigations of high-temperature corrosion phenomena in straw-fired boilers. Energy Fuels 1999;13(6):1114–21. http://dx.doi.org/10.1021/ef990001g.

[30] Li YS, Niu Y, Wu WT. Accelerated corrosion of pure Fe, Ni, Cr and several Fe-based alloys induced by $ZnCl_2$–KCl at 450 °C in oxidizing environment. Mater Sci Eng A 2003;345(1–2):64–71. http://dx.doi.org/10.1016/S0921-5093(02)00386-6.

[31] Nielsen HP, Frandsen FJ, Dam-Johansen K, Baxter LL. The implications of chlorine-associated corrosion on the operation of biomass-fired boilers. Prog Energy Combust Sci 2000;26(3):283–98. http://dx.doi.org/10.1016/S0360-1285(00)00003-4.

[32] Phase diagrams for ceramists. Columbus, Ohio, USA: American Ceramic Society; 1996. Part XII 1996.

[33] Folkeson N, Jonsson T, Halvarsson M, Johansson LG, Svensson JE. The influence of small amounts of KCl(s) on the high temperature corrosion of a Fe–2.25Cr–1Mo steel at 400 and 500 °C. Mater Corros 2011;62(7):606–15. http://dx.doi.org/10.1002/maco.201005942.

[34] Grabke HJ, Reese E, Spiegel M. The effects of chlorides, hydrogen chloride, and sulfur dioxide in the oxidation of steels below deposits. Corros Sci 1995;37(7):1023–43. http://dx.doi.org/10.1016/0010-938X(95)00011-8.

[35] Stemmler M, Müller M. Chemical hot gas cleaning concept for the “CHRISGAS” process. Biomass Bioenergy 2011;35(1):105–15. http://dx.doi.org/10.1016/j.biombioe.2011.03.044.